

Intrinsic Triple Order in A-site Columnar-ordered Quadruple Perovskites: Proof of Concept

Alexei A. Belik,^[a] Dmitry D. Khalyavin,^[b] Lei Zhang,^[a,c] Yoshitaka Matsushita,^[d] Yoshio Katsuya,^[e] Masahiko Tanaka,^[e] Roger D. Johnson,^[f] and Kazunari Yamaura^[a,c]

Abstract: There is an emerging topic in the science of perovskite materials: A-site columnar-ordered $A_2A'A''B_4O_{12}$ quadruple perovskites, which have an intrinsic triple order at the A sites. However, in many examples reported so far, A' and A'' cations are the same, and the intrinsic triple order is hidden. Here, we investigate structural properties of $Dy_2CuMnMn_4O_{12}$ (1) and $Ho_2MnGaMn_4O_{12}$ (2) by neutron and X-ray powder diffraction and prove the triple order at the A sites. The cation distributions determined are $[Ho_2]_A[Mn]_{A'}[Ga_{0.66}Mn_{0.34}]_{A''}[Mn_{3.66}Ga_{0.34}]_B O_{12}$ and $[Dy_2]_A[Cu_{0.73}Mn_{0.27}]_{A'}[Mn_{0.80}Dy_{0.20}]_{A''}[Mn_{1.89}Cu_{0.11}]_B [Mn_2]_{B_2} O_{12}$. There are clear signatures of Jahn-Teller distortions in 1 and 2, and the orbital pattern is combined with an original type of charge ordering in 1. Columnar-ordered quadruple perovskites represent a new playground to study complex interactions between different electronic degrees of freedom. No long-range magnetic order was found in 2 by neutron diffraction, and its magnetic properties in low fields are dominated by an impurity with negative magnetization or magnetization reversal. On the other hand, 1 shows three magnetic transitions at 21, 125, and 160 K.

The ABO_3 perovskite structure, built from corner-shared BO_6 octahedra with cavities filled by A, is remarkably versatile.^[1] It is said that nearly every element (but, more precisely, metal) in the

periodic table can be inserted into the A and/or B sites. The versatility originates from the ability of BO_6 octahedra to rotate in different manners and adjust the sizes of cavities to the size and number of different A cations. The rotations of BO_6 octahedra are usually described by the Glazer tilt system and B-O-B bond angles,^[2] and there are basically 15 tilt systems in ABO_3 perovskites.^[3] The other versatility can originate from the presence and ordering of oxygen vacancies (but sometimes cation vacancies), which, in turn, can drive different cation orders.^[3,4]

In oxygen and cation stoichiometric perovskites, different A and B cations can be distributed randomly in the A and B sites or can form different short-range and long-range ordered structures. There exists the 1:1, 1:2 and 1:3 B-site and A-site ordered structures (a higher degree of ordering is extremely rare).^[4] In the 1:1 cases, cations can order in the rock salt, columnar, or layered manners.^[4] Among B-site-ordered structures, the 1:1 rock salt ordering of $A_2BB'O_6$ double perovskites is dominant:^[4] about one thousand of such perovskites have been reported.^[5] Among A-site-ordered structures, the 1:3 body-centered^[4] ordering of $AA'_3B_4O_{12}$ quadruple perovskites is dominant.^[4,6,7] There are possibilities of simultaneous ordering at the A and B sites as in the so-called doubly ordered^[4] (or double double)^[8,9] perovskites $AA'BB'O_6$ ^[10] and in $AA'_3B_2B'_2O_{12}$ quadruple perovskites.^[11]

There are four Glazer octahedral tilt systems that result in A-site ordering: $a^+a^+a^+$ (1:3), $a^+a^+c^-$ (1:1:2), $a^0b^+b^+$ (1:1:2) and $a^0b^+b^-$ (1:1),^[4,6] where numbers in parenthesis give the number and ratio among non-equivalent A sites. [Note that $a^+b^+c^+$ and $a^+b^-c^-$ tilts can also formally give A-site ordering;^[3] however, they present small deviations from the $a^+a^+a^+$ and $a^+b^-b^-$ tilts.] These numbers show that the $a^+a^+c^-$ (1:1:2) and $a^0b^+b^+$ (1:1:2) tilt systems could produce intrinsic triple orders at the A sites. However, no compounds with the $a^0b^+b^+$ (1:1:2) tilt system (and also with the $a^0b^+b^-$ (1:1) tilt system) have been reported.^[4] The $a^+a^+a^+$ (1:3) tilt system results in the A-site-ordered $AA'_3B_4O_{12}$ quadruple perovskites with a twelve-fold coordinated A site and a square-planar coordinated A' site.^[4,7] The $a^+a^+c^-$ (1:1:2) tilt system results in the so-called A-site columnar-ordered $A_2A'A''B_4O_{12}$ quadruple perovskites with a ten-fold coordinated A site, a square-planar coordinated A' site, and a tetrahedrally coordinated A'' site (Figures 1 and S1).^[12] However, in the majority of examples reported so far, A' and A'' cations are the same ($A' = A''$), and the intrinsic triple order is hidden, for example, in $CaFeTi_2O_6$,^[13] $CaMnTi_2O_6$,^[14] $RMnMnSbO_6$ ($R = La, Pr, Nd$ and Sm),^[8] $RMnGaTiO_6$ ($R = Sm$ and Gd),^[15] $RMnMn_2O_6 \equiv RMn_3O_6$ ($R = Gd-Tm$ and Y),^[16] $CaMnFeReO_6$ ^[9] and $CaMnMnReO_6$,^[9] where short formula look like double perovskites. There is only one example where A' and A'' cations are different, $Ca_2CuMnFe_2Re_2O_{12}$, and this compound shows a partial ordering of Cu^{2+} and Mn^{2+} between the A' and A'' sites.^[9] There is also an example where the same cation ($A' = A'' = Mn$) has different oxidation states at the A' and A'' sites, $[R^{3+}_2]_A[Mn^{3+}]_{A'}[Mn^{2+}]_{A''}[Mn^{3+}_2]_{B_1}[Mn^{3+}Mn^{4+}]_{B_2}O_{12}$.^[16]

In this work, we report on the synthesis, crystal structures, and

- [a] Dr. A. A. Belik, L. Zhang, Dr. K. Yamaura
Research Center for Functional Materials, National Institute for Materials Science (NIMS), 1-1 Namiki, Tsukuba, Ibaraki 305-0044 (Japan)
Fax: (+81) 29-860-4674
E-mail: Alexei.Belik@nims.go.jp
- [b] Dr. D. D. Khalyavin
ISIS Facility, Rutherford Appleton Laboratory, Harwell Oxford, Didcot OX11 0QX, United Kingdom
- [c] L. Zhang, Dr. K. Yamaura
Graduate School of Chemical Sciences and Engineering, Hokkaido University, North 10 West 8, Kita-ku, Sapporo, Hokkaido 060-0810, Japan
- [d] Dr. Y. Matsushita
Material Analysis Station, National Institute for Materials Science (NIMS), Sengen 1-2-1, Tsukuba, Ibaraki 305-0047, Japan
- [e] Dr. Y. Katsuya, Dr. M. Tanaka
Synchrotron X-ray Station at SPring-8, NIMS, Kouto 1-1-1, Sayo-cho, Hyogo 679-5148, Japan
- [f] Dr. R. D. Johnson
Department of Physics, University of Oxford, Clarendon Laboratory, Parks Road, Oxford, OX1 3PU, United Kingdom

Supporting information for this article is available on the WWW under <http://dx.doi.org/> or from the author.

materials properties of other members of the $A_2A'A''B_4O_{12}$ quadruple perovskite family: $Dy_2CuMnMn_4O_{12}$ and $Ho_2MnGaMn_4O_{12}$, where we aimed at inserting Cu^{2+} into the square-planar A' site and Ga^{3+} into the tetrahedral A'' site, respectively. Using a combination of X-ray and neutron diffraction data we showed that there is a significant amount of Cu^{2+} at the A' site but no Cu^{2+} at the A'' site, and there is a significant amount of Ga^{3+} at the A'' site but no Ga^{3+} at the A' site. These facts prove the intrinsic nature of the A-site triple order in such perovskites and provide a new playground for manipulation of structural and physical properties through selective cation substitutions.

$Dy_2CuMnMn_4O_{12}$ and $Ho_2MnGaMn_4O_{12}$ were prepared by a high-pressure high-temperature method at 6 GPa and about 1550 K for 2 h in Au capsules ($Ho_2MnGaMn_4O_{12}$) and about 1670 K for 2 h in Pt capsules ($Dy_2CuMnMn_4O_{12}$) in a belt-type high-pressure apparatus. We emphasize that the high-pressure high-temperature method is an essential tool for the preparation of most A-site-ordered quadruple perovskites.^[4,12] $Ho_2MnGaMn_4O_{12}$ (space group $P4_2/nmc$, $a = 7.3630(1)$ Å and $c = 7.7517(1)$ Å at room temperature (RT)) contained about 2 wt. % of $(Ho_{0.8}Mn_{0.2})MnO_3$ impurity. $Dy_2CuMnMn_4O_{12}$ (space group $Pmmn$, $a = 7.28230(1)$ Å, $b = 7.35069(1)$ Å, $c = 7.82259(1)$ Å at RT) contained about 5.2 wt. % of $Dy(Cu_{1.6}Mn_{1.4})Mn_4O_{12}$ impurity. The cation distribution was determined using synchrotron and neutron powder diffraction methods. Very different coherent neutron scattering lengths of Mn, Ga, and Cu allowed the precise determination of cation distributions. The cation distributions determined are $[Ho^{3+}_2]_A[Mn^{3+}]_{A'}[Ga^{3+}_{0.66}Mn^{2+}_{0.34}]_{A''}[Mn^{3+}_{3.66}Ga^{3+}_{0.34}]_B O_{12}$ and $[Dy^{3+}_2]_A[Cu^{2+}_{0.73}Mn^{3+}_{0.27}]_{A'}[Mn^{2+}_{0.80}Dy^{3+}_{0.20}]_{A''}[Mn^{3+}_{1.89}Cu^{2+}_{0.11}]_B O_{12}$. Details of the refinement procedures and results are given in Supporting Information (Tables S1-S4 and Figures S1-S4). As the impurity in $Dy_2CuMnMn_4O_{12}$ is (Cu,Mn)-rich, the main phase should be Dy-rich. Our structural analysis with neutron diffraction confirmed this and gave the following composition of the main perovskite phase: $Dy_{2.2}Cu_{0.85}Mn_{4.95}O_{12}$. Synthesis conditions (such as, pressure, annealing temperature, and cooling rates) should, of course, have effects on the degree of cation ordering as was found in $Ca_2CuMnFe_2Re_2O_{12}$.^[9] However, the general tendency should be primarily determined by the cation nature, size, and coordination preferences.^[12]

As tetrahedral sites are highly unfavourable for Mn^{3+} we assumed that Mn at the tetrahedral A'' site has the oxidation state +2 in the above cation distribution formula. The bond valence sum (BVS)^[17] values of Ga^{3+} are reduced because of the presence of Mn^{2+} in the A'' site that increases the observed A'' -O bond lengths. The BO_6 octahedron in $Ho_2MnGaMn_4O_{12}$ has a noticeable Jahn-Teller distortion (with the distortion parameter $\Delta = 7.7 \times 10^{-4}$) with the longest Mn3-O3 bond distance tilted away from the c -axis by $\sim 20^\circ$ due to the heavy octahedral tilting. The presence of cooperative Jahn-Teller distortions is caused by a large concentration of Jahn-Teller active Mn^{3+} cations at the B site, and the observed orbital pattern (Figure 1) is a rare example of the ferro-orbital ordering previously reported for only $La_{0.5}Ba_{0.5}CoO_3$ perovskite.^[18]

As it was expected from the crystallographic considerations,^[12] Ga^{3+} was not found at the square-planar A' site. Distribution of Ga^{3+} occurs between the tetrahedral A'' site and octahedral B site with the preferred occupation of the A'' site (with about 2:1 (A'' :B) ratio). If this tendency continues the Ga:Mn ratio at the A'' site can be increased in solid solutions $Ho_2Mn_{6-x}Ga_xO_{12}$ with the increase of the Ga content. In principle, such solid solutions should exist from $x = 0$ to $x = 5$, that is, from $Ho_2MnMnMn_4O_{12}$ ^[16] to $Ho_2MnGaGa_4O_{12}$

(with the A'' site fully occupied by Ga^{3+}). We could prepare such solid solutions up to $x = 4$ at 6 GPa and about 1470-1570 K for 2 h in Au capsules (with $a = 7.3641(1)$ Å and $c = 7.7152(1)$ Å for $x = 2$, $a = 7.3640(1)$ Å and $c = 7.6750(1)$ Å for $x = 3$, and $a = 7.3689(1)$ Å and $c = 7.6173(1)$ Å for $x = 4$ at RT (Table S5)). $Ho_2MnGaGa_4O_{12}$ (with $a = 7.3773(1)$ Å and $c = 7.5719(1)$ Å at RT) contained a lot of impurities: $HoGaO_3$ (~ 17 wt. %), Ga_2O_3 (~ 19 wt. %), and $Ho_3Ga_5O_{12}$ (~ 3 wt. %), but lattice parameters of the $Ho_2Mn_{6-x}Ga_xO_{12}$ -type phase continued to change monotonically (Figure S5) suggesting that the chemical composition of that phase could be close to $Ho_2MnGaGa_4O_{12}$.

The Mn3 site (B1) of $Dy_2CuMnMn_4O_{12}$ shows a strong Jahn-Teller distortion - this could be a reason why a small fraction of Jahn-Teller Cu^{2+} cations is also located in this site together with Jahn-Teller Mn^{3+} cations. On the other hand, there are no Cu^{2+} cations in the Mn4 site (B2), which has a more regular octahedral coordination. The BVS calculations reveal a clear charge disproportionation between the manganese in the B1 and B2 positions, with oxidation states +3.17(1) and +3.76(1) (from the neutron refinement), respectively. Thus the cooperative Jahn-Teller effect in $Dy_2CuMnMn_4O_{12}$ is conjugated with charge ordering phenomena, where the layers of strongly elongated $Mn^{3+}O_6$ octahedra are interchanged with nearly regular $Mn^{4+}O_6$ octahedral layers along the c -axis of the $Pmmn$ orthorhombic structure (Figure 1b). To the best of our knowledge, this is the first example of charge and ferro-orbital layer-type patterns observed in complex perovskite oxides, which indicates that this class of columnar-ordered quadruple manganites provides a new playground to study interplay between the charge and orbital degrees of freedom. It is well known that cooperation of these degrees of freedom with the magnetic subsystem in simple charge-doped manganites results in a variety of interesting phenomena such as metal insulator transitions and giant magnetoresistance.^[19] Thus, a systematic investigation of physical properties and magnetic structures of such novel A-site ordered perovskites with different degree of charge doping is a promising avenue for future studies. It is known that cation ordering/disordering could have dramatic effects on properties of perovskite materials.^[4,20,21]

Figure 2 depicts dc magnetic susceptibilities of $Ho_2MnGaMn_4O_{12}$. At $H = 100$ Oe (Figure S6a), some magnetic anomalies are seen at 27 K and 73 K on zero-field-cooled (ZFC) and field-cooled on cooling (FCC) curves. Moreover, negative magnetization or magnetization reversal was observed below about 10 K on the 100 Oe FCC curve. All these features resemble magnetic behaviours of $(Ho_{0.8}Mn_{0.2})MnO_3$ (Figure S6b) and $(Tm_{0.667}Mn_{0.333})MnO_3$.^[22] Therefore, we conclude that the magnetic response in small magnetic fields is dominated by $(Ho_{0.8}Mn_{0.2})MnO_3$ ferrimagnetic impurity. At a high magnetic field of 10 kOe, no anomalies were observed except the divergence between the ZFC and FCC curves near 7 K.

No specific heat anomalies at $H = 0$ Oe and 90 kOe (Figure S13a) and no evidence for magnetic Bragg scattering in the neutron diffraction experiment at $T = 1.5$ K (Figure S2) were found for $Ho_2MnGaMn_4O_{12}$, suggesting the absence of a long-range magnetic order. However, a high magnetic field of 90 kOe had an effect on the specific heat below about 100 K. This fact shows that short-range magnetic correlations should be present at this temperature, and this conclusion is further supported by a strong magnetic diffuse scattering observed in the low-temperature ($T = 1.5$ K) neutron diffraction pattern (Figure S2a, inset). M versus H curves at 5 K show an S-type shape with small hysteresis near the origin that is typical for spin glasses (Figure S13b). At 20 K, the hysteresis on M

versus H curves almost disappeared. Therefore, neutron diffraction and magnetic data are consistent with each other. Physical properties of $\text{Ho}_2\text{Mn}_{6-x}\text{Ga}_x\text{O}_{12}$ are reported on Figures S6-S15. For example, clear features of a spin-glass (SG) transition were observed in $\text{Ho}_2\text{MnGa}(\text{MnGa}_3)\text{O}_{12}$ ($x = 4$) at $T_{\text{SG}} = 11\text{--}12\text{ K}$.

The absence of a long-range magnetic order in $\text{Ho}_2\text{MnGaMn}_4\text{O}_{12}$ is surprising because the B site is only diluted by 9 % with non-magnetic Ga^{3+} cations (and the B site should also contain about 9 % of Mn^{4+}). Such dilution in LaMnO_3 produces just minor effects.^[23,24] Undoped o-HoMnO_3 ^[25] and $\text{Ho}_{2-x}\text{MnMnMn}_4\text{O}_{12-1.5x}$ ($= \text{Ho}_{1-y}\text{Mn}_3\text{O}_{6-1.5y}$)^[16] perovskites show complex magnetic behaviours with several transition temperatures. Peculiar magnetic behavior of $\text{Ho}_2\text{MnGaMn}_4\text{O}_{12}$ can be caused by the fact that the BO_6 network in A-site columnar-ordered quadruple perovskites is intrinsically highly tilted. The Mn-O-Mn bond angles of $133\text{--}145^\circ$ (Table S2) deviate strongly from 180° and reduce the nearest-neighbor exchange interactions between Mn cations and introduce competition with next-nearest-neighbor exchange interactions. This interaction reduction and increased frustration coupled with the presence of small cation disorder seems to be enough to completely suppress a long-range order.

On the other hand, specific heat and magnetic measurements showed that $\text{Dy}_2\text{CuMnMn}_4\text{O}_{12}$ shows three long-range magnetic order transitions at $T_{\text{N}3} = 21\text{ K}$, $T_{\text{N}2} = 125\text{ K}$, and $T_{\text{N}1} = 160\text{ K}$ (Figure 3). The intrinsic nature of the three phase transitions is further supported by the fact that all $\text{R}_2\text{CuMnMn}_4\text{O}_{12}$ ($\text{R} = \text{Dy-Lu}$ and Y) exhibit similar magnetic properties and systematic changes of phase transition temperatures.^[12]

In conclusion, we synthesized A-site columnar-ordered $\text{A}_2\text{A}'\text{A}''\text{B}_4\text{O}_{12}$ quadruple perovskites $\text{Dy}_2\text{CuMnMn}_4\text{O}_{12}$ and $\text{Ho}_2\text{MnGaMn}_4\text{O}_{12}$ and investigated their structural properties by means of neutron and X-ray powder diffraction. We found that there is a significant amount of Cu^{2+} at the square-planar A' site but no Cu^{2+} at the tetrahedral A'' site, and there is a significant amount of Ga^{3+} at the A'' site but no Ga^{3+} at the A' site. Therefore, we proved that $\text{Dy}_2\text{CuMnMn}_4\text{O}_{12}$ and $\text{Ho}_2\text{MnGaMn}_4\text{O}_{12}$ have a triple cation order at the A sites. $\text{Ho}_2\text{MnGaMn}_4\text{O}_{12}$ is a rare example of a perovskite with small Ga^{3+} cations at the A sites. In addition, our structural analysis revealed that both perovskites exhibit significant Jahn-Teller distortions of the octahedra coordinating B site manganese. A long-range character of the distortions results in a rare example of ferro-orbital ordering in $\text{Ho}_2\text{MnGaMn}_4\text{O}_{12}$. In the case of $\text{Dy}_2\text{CuMnMn}_4\text{O}_{12}$, the cooperative Jahn-Teller lattice distortion is combined with charge ordering, resulting in an original layer-type charge and orbital pattern. The latter compound also exhibits three distinct magnetic phases, which might reflect a complex character of interaction between the magnetic and electronic subsystems. Thus, our results demonstrate that the A-site columnar-ordered manganites provide a new avenue to study interplay between charge, spin, and orbital degrees of freedom.

Acknowledgements

This work was supported by JSPS KAKENHI Grant Numbers JP15K14133 and JP16H04501 and JSPS Bilateral Open Partnership Joint Research Projects. R.D.J. acknowledges support from a Royal Society University Research Fellowship. D.D.K acknowledges TUMOCs project. This project has received funding from the European Union's Horizon 2020 research and innovation programme under the Marie Skłodowska-Curie Grant Agreements No. 645660. The synchrotron radiation experiments were performed at the SPring-8 with the approval of NIMS Synchrotron X-ray Station (Proposal Number: 2017B4502).

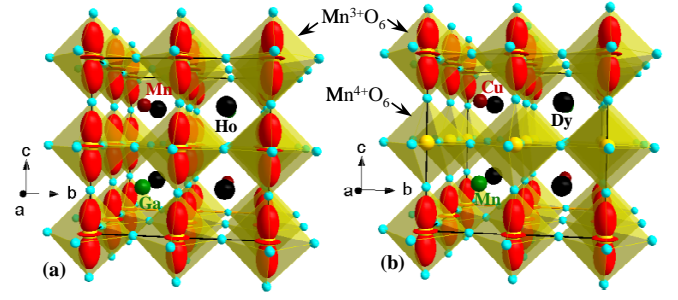


Figure 1. Orbital ordering patterns in (a) $\text{Ho}_2\text{MnGaMn}_4\text{O}_{12}$ and (b) $\text{Dy}_2\text{CuMnMn}_4\text{O}_{12}$ (to clearly demonstrate the ferro-type of the orbital patterns, the octahedral tilting was omitted from the structures).

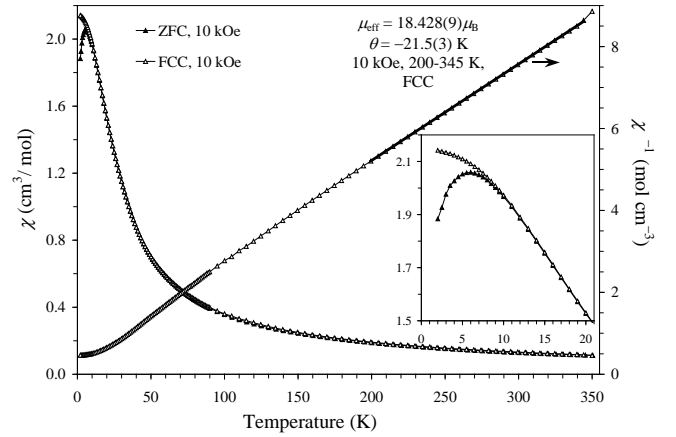


Figure 2. ZFC (filled symbols) and FCC (empty symbols) dc magnetic susceptibility ($\chi = M/H$) curves of $\text{Ho}_2\text{MnGaMn}_4\text{O}_{12}$ at 10 kOe (left-hand axis). The right-hand axis shows the inverse FCC 10 kOe curve with Curie-Weiss fitting results. The inset shows a fragment of the ZFC and FCC χ versus T curves at $H = 10\text{ kOe}$.

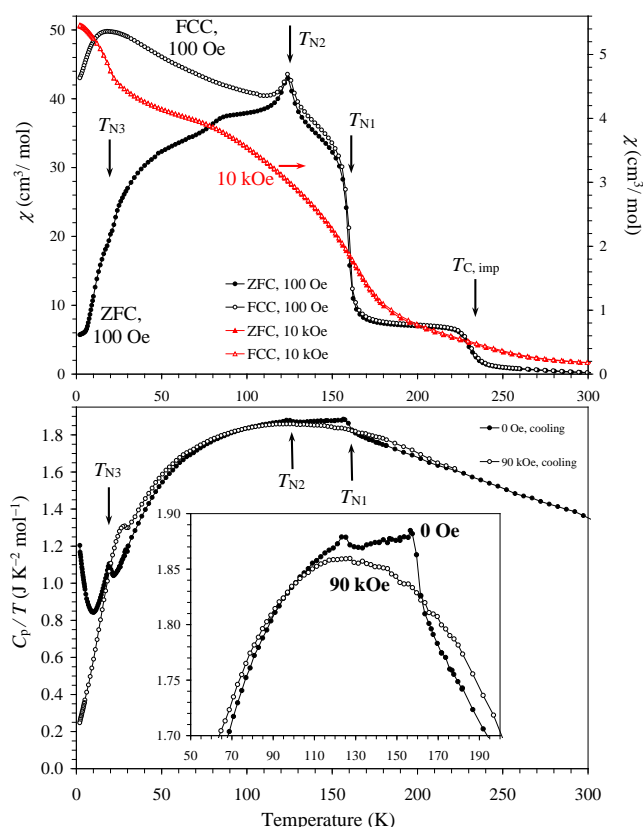


Figure 3. (a) ZFC (filled symbols) and FCC (empty symbols) dc magnetic susceptibility ($\chi = M/H$) curves of $\text{Dy}_2\text{CuMnMn}_4\text{O}_{12}$ at $H = 100$ Oe (left-hand axis; circles) and 10 kOe (right-hand axis; red triangles). (b) Specific heat of $\text{Dy}_2\text{CuMnMn}_4\text{O}_{12}$ at $H = 0$ Oe (on cooling; black circles) and 90 kOe (on cooling; white circles) plotted as C_p/T versus T ; the inset depicts details. Arrows show magnetic transition temperatures, where $T_{C, \text{imp}}$ denotes an anomaly from the $\text{Dy}(\text{Cu}_{1.6}\text{Mn}_{1.4})\text{Mn}_4\text{O}_{12}$ impurity.

- [1] R. H. Mitchell, *Perovskites: Modern and Ancient*; Almaz Press: Thunder Bay, Ontario, Canada, 2002.
- [2] A. M. Glazer, *Acta Crystallogr., Sect. A* **1975**, *31*, 756.
- [3] A. M. Abakumov, A. A. Tsirlin, E. V. Antipov, *Transition-Metal Perovskites. In Comprehensive Inorganic Chemistry II (Second Edition): From Elements to Applications*, eds. Reedijk, J.; Poeppelmeier, K. R. Elsevier: Amsterdam, 2013, Vol. 2, pp. 1–40.
- [4] G. King, P. M. Woodward, *J. Mater. Chem.* **2010**, *20*, 5785.
- [5] S. Vasala, M. Karppinen, *Prog. Solid State Chem.*, **2015**, *43*, 1.
- [6] J.-H. Park, P. M. Woodward, J. B. Parise, *Chem. Mater.* **1998**, *10*, 3092.
- [7] A. N. Vasil'ev, O. S. Volkova, *Low Temp. Phys.* **2007**, *33*, 895.
- [8] E. Solana-Madruga, A. M. Arevalo-Lopez, A. J. Dos Santos-Garcia, E. Urones-Garrote, D. Avila-Brande, R. Saez-Puche, J. P. Attfield, *Angew. Chem. Int. Ed.* **2016**, *55*, 9340.
- [9] G. M. McNally, A. M. Arévalo-López, P. Kearins, F. Orlandi, P. Manuel, J. P. Attfield, *Chem. Mater.* **2017**, *29*, 8870.
- [10] M. C. Knapp, P. M. Woodward, *J. Solid State Chem.* **2006**, *179*, 1076.
- [11] S.-H. Byeon, S.-S. Lee, J. B. Parise, P. M. Woodward, N. H. Hur, *Chem. Mater.* **2005**, *17*, 3552.
- [12] A. A. Belik, *Dalton Trans.* **2018**, *47*, 3209.
- [13] K. Leinenweber, J. Parise, *J. Solid State Chem.* **1995**, *114*, 277.
- [14] A. Aimi, D. Mori, K. Hiraki, T. Takahashi, Y. J. Shan, Y. Shirako, J. S. Zhou, Y. Inaguma, *Chem. Mater.* **2014**, *26*, 2601.
- [15] G. Shimura, K. Niwa, Y. Shirako, M. Hasegawa, *Eur. J. Inorg. Chem.* **2017**, 835.
- [16] L. Zhang, Y. Matsushita, K. Yamaura, A. A. Belik, *Inorg. Chem.* **2017**, *56*, 5210.
- [17] N. E. Brese, M. O'Keeffe, *Acta Crystallogr., Sect. B: Struct. Sci.* **1991**, *47*, 192.
- [18] F. Fauth, E. Suard, V. Caignaert, *Phys. Rev. B: Condens. Matter Mater. Phys.* **2001**, *65*, 060401.
- [19] M. B. Salamon, M. Jaime, *Rev. Mod. Phys.* **2001**, *73*, 583.
- [20] J. Young, E. J. Moon, D. Mukherjee, G. Stone, V. Gopalan, N. Alem, S. J. May, J. M. Rondinelli, *J. Am. Chem. Soc.* **2017**, *139*, 2833.
- [21] T. Ferreira, D. Carone, A. Huon, A. Herklotz, S. A. Stoian, S. M. Heald, G. Morrison, M. D. Smith, H.-C. zur Loye, *Inorg. Chem.* **2018**, *57*, 7362.
- [22] L. Zhang, D. Gerlach, A. Dönni, T. Chikyow, Y. Katsuya, M. Tanaka, S. Ueda, K. Yamaura, A. A. Belik, *Inorg. Chem.* **2018**, *57*, 2773.
- [23] J. Blasco, J. Garcia, J. Campo, M. C. Sanchez, G. Subias, *Phys. Rev. B: Condens. Matter Mater. Phys.* **2002**, *66*, 174431.
- [24] J. B. Goodenough, R. I. Dass, J. S. Zhou, *Solid State Sci.* **2002**, *4*, 297.
- [25] A. Minoz, M. T. Casais, J. A. Alonso, M. J. Martinez-Lope, J. L. Martinez, M. T. Fernandez-Diaz, *Inorg. Chem.* **2001**, *40*, 1020.

Received: ((will be filled in by the editorial staff))

Published online on ((will be filled in by the editorial staff))

Keywords: high-pressure chemistry • materials science • perovskite phases

